

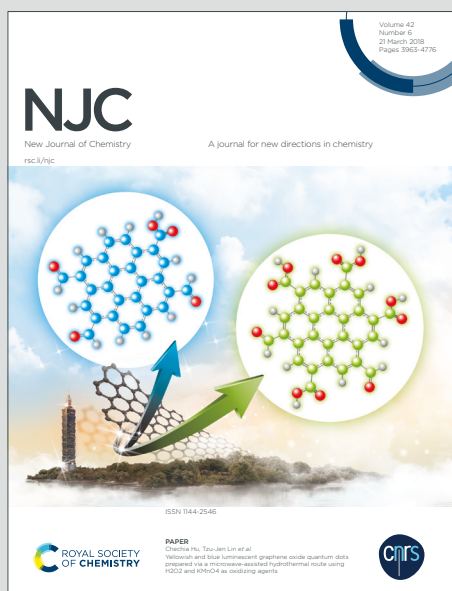
# NJC

New Journal of Chemistry

Accepted Manuscript

A journal for new directions in chemistry

This article can be cited before page numbers have been issued, to do this please use: S. Pramanik, S. K. Manna, S. Pathak, D. Mandal, K. Pal and S. Mukhopadhyay, *New J. Chem.*, 2020, DOI: 10.1039/D0NJ02117B.



This is an Accepted Manuscript, which has been through the Royal Society of Chemistry peer review process and has been accepted for publication.

Accepted Manuscripts are published online shortly after acceptance, before technical editing, formatting and proof reading. Using this free service, authors can make their results available to the community, in citable form, before we publish the edited article. We will replace this Accepted Manuscript with the edited and formatted Advance Article as soon as it is available.

You can find more information about Accepted Manuscripts in the [Information for Authors](#).

Please note that technical editing may introduce minor changes to the text and/or graphics, which may alter content. The journal's standard [Terms & Conditions](#) and the [Ethical guidelines](#) still apply. In no event shall the Royal Society of Chemistry be held responsible for any errors or omissions in this Accepted Manuscript or any consequences arising from the use of any information it contains.

Cite this: DOI: 10.1039/c0xx00000x

Dynamic Article Links ►

www.rsc.org/xxxxxx

## ARTICLE TYPE

**Chromogenic and fluorogenic “off-on-off” chemosensor for selective and sensitive detection of aluminum (Al<sup>3+</sup>) and bifluoride (HF<sub>2</sub><sup>-</sup>) ions in solution and in living HepG2 cells: synthesis, experimental and theoretical studies**Samit Pramanik,<sup>a</sup> Saikat Kumar Manna,<sup>b</sup> Sudipta Pathak,<sup>b,\*</sup> Debasish Mondal,<sup>c</sup> Kunal Pal,<sup>d</sup> and Subrata Mukhopadhyay<sup>a</sup>

Received (in XXX, XXX) Xth XXXXXXXXXX 20XX, Accepted Xth XXXXXXXXXX 20XX

DOI: 10.1039/b000000x

A simple pyridine-dicarbohydrazide based colorimetric and fluorometric chemosensor **L** was designed and synthesized for Al<sup>3+</sup> ions sensing in organo aqueous solution. In presence of Al<sup>3+</sup> ions, probe **L** exhibited visible color changes and fluorescence enhancement (20-fold) due to Al<sup>3+</sup> induced chelation-enhanced fluorescence (CHEF) effects. The chemosensor **L** revealed high selectivity toward Al<sup>3+</sup> ions by “turn-on” fluorescence among the other competitive metal ions examined with a detection limit of 0.8 μM. The probe **L** was found to bind with Al<sup>3+</sup> ions in a 1: 2 (probe: metal) stoichiometric fashion, with the association constant (K<sub>a</sub>) of 4.26 × 10<sup>4</sup> M<sup>-1</sup>. In addition, DFT and TDDFT calculations were carried out to recognize the binding nature and electronic properties of the probe **L** and its Al-complex. Furthermore, *in situ* prepared [L-Al] complex was able to detect HF<sub>2</sub><sup>-</sup> anions via a metal displacement strategy. The bioimaging application of Al<sup>3+</sup> and HF<sub>2</sub><sup>-</sup> were implemented in the living human liver cancer cells (Hep G2).

**Introduction**

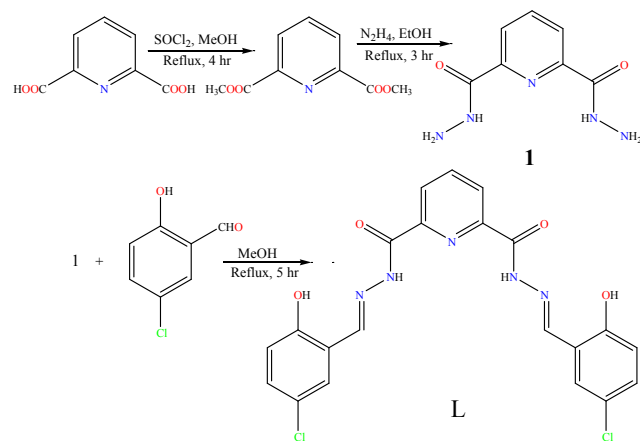
Being the third most abundant (8.3% by weight) element (after oxygen and silicon) on the surface of the earth, aluminum is widely attached with our daily contemporary life in the form of food packaging, water purification, cooking utensils, pharmaceuticals, manufacturing of computers, *etc.*<sup>1-3</sup> Aluminium compounds are also extensively used in paper industry, in dye production, in textile industry, as a component of many cosmetic preparations and currently utilized in alimentary industry and in many more.<sup>4-5</sup> Therefore, there is a good chance of accumulation of aluminum ion (Al<sup>3+</sup>) in food chain and toxicity towards human health. But, the tolerable daily intake of aluminum is about (3–10) mg and consequently upper limit of aluminum nutritional intake is about 7 mg/kg<sup>-1</sup> per week of the body weight according to the WHO report.<sup>6</sup> Excess accumulation of this metal causes some serious diseases like myopathy, Parkinson’s disease, Alzheimer’s disease, osteoporosis, headaches, anemia, chronic renal failure, dialysis encephalopathy, bone softening, kidney damage and even breast cancer.<sup>7-9</sup> The solubility of aluminium minerals at lower pH increases the amount of available Al<sup>3+</sup>, which can affect plant’s normal growth and development, ultimately hampering agricultural production.<sup>10</sup> Therefore, easy

detection of aluminum ion is imperative in various samples connected to environment, foodstuff, medicine, *etc.* But detection of aluminium ion is still a major challenge due to its low coordination capability, high hydration aptitude and the lack of spectroscopic features.<sup>11</sup> A number of analytical techniques have been used for the detection of aluminum ions, such as atomic absorption spectrometry,<sup>12</sup> inductively coupled plasma atomic emission spectrometry (ICP-AES),<sup>13-14</sup> inductively coupled plasma mass spectrometry (ICP-MS),<sup>15</sup> nanoparticle-based sensors,<sup>16</sup> ion selective membrane,<sup>17</sup> electrochemical methods,<sup>18</sup> and several other methods.<sup>19</sup> But these techniques are restricted to the laboratory because of high equipment cost, time consuming and necessity for trained personnel. However, spectrofluorimetry is superior in terms of quick analysis, high selectivity, sensitivity and ease of operation. As Al<sup>3+</sup> is a hard acid, it prefers hard base donor sites for coordination,<sup>20</sup> so the Schiff base probes with N and O donor centres could be used as good ligands for Al<sup>3+</sup> detection.<sup>21</sup> In several research fields hydrazides have been extensively used as ligands due to their facile syntheses, tunable electronic properties and good chelating capability.<sup>22</sup> In this work, we have designed and synthesized a pyridine-dicarbohydrazide based ‘turn-on’ chemosensors **L** which show high selectivity for Al<sup>3+</sup> with low detection limit (LOD).

Anions play a vital role in the area of supramolecular chemistry, especially in environmental, chemical, medical and biological systems. Among the different anions, the semi-ionic, three-center, and four-electron bonding bifluoride ions ( $\text{HF}_2^-$ ) recognition is of growing interest because of its extensive applications in various fields including etching of borosilicates glass capillary columns, insecticides, fluorometric detection of ultra-trace levels of beryllium in occupational hygiene samples, preparation of borane derivatives and molten salts.<sup>23</sup> Until now, a very few chemosensors have been reported for bifluoride ions.<sup>24</sup> Therefore, it is an urgent requirement for fluorescent and biocompatible probes that can selectively and sensitively detect bifluoride ions with rapid response through easy spectral analysis. However, the design and development of fluorescent chemosensors for anions in aqueous solution is still a difficult task due to strong hydration properties of anions. This problem could be evaded by using the metal displacement strategy. Keeping this in mind, we report here a displacement-based sensing system by using  $\text{Al}^{3+}$ -based ensemble ( $\text{L}-2\text{Al}^{3+}$ ) for bifluoride ions recognition. It is noteworthy to mention that the chemosensor **L** has interesting analytical features like its easy synthetic route with good yield and reasonably low detection limit for  $\text{Al}^{3+}$  ion with no interference from a number of cations in comparison to reported methods (Table S1, ESI<sup>†</sup>). Another notable aspect of  $\text{L}-2\text{Al}^{3+}$  complex is that it displays a good reversible fluorescence response to  $\text{HF}_2^-$ . Furthermore, probe **L** is effectively applied to image  $\text{Al}^{3+}$  and  $\text{HF}_2^-$  ions in cultured HepG2 cells.

## Results and discussion

**Scheme 1** outlined the synthetic route of chemosensor **L**. Compound **1** was prepared following literature procedure.<sup>25</sup> The probe **L** was then synthesized by the condensation reaction between compound **1** and 2-hydroxy-4-chlorobenzaldehyde with 84% yield. The molecular structure of **L** was confirmed by  $^1\text{H}$  NMR,  $^{13}\text{C}$  NMR, ESI-MS, FT-IR and also by single-crystal X-ray diffraction analysis (Fig. 1, Table S2, ESI<sup>†</sup>).



**Scheme 1** Chemical structure and synthetic route of **L**.

The spectroscopic properties of the probe **L** were investigated by monitoring absorption and fluorescence changes in presence of several metal ions, such as  $\text{K}^+$ ,  $\text{Na}^+$ ,  $\text{Mg}^{2+}$ ,  $\text{Ca}^{2+}$ ,  $\text{Pb}^{2+}$ ,  $\text{Pd}^{2+}$ ,  $\text{Cd}^{2+}$ ,  $\text{Hg}^{2+}$ ,  $\text{Zn}^{2+}$ ,  $\text{Cu}^{2+}$ ,  $\text{Al}^{3+}$ ,  $\text{Ag}^+$ ,  $\text{Fe}^{2+}$ ,  $\text{Co}^{2+}$ ,  $\text{Ni}^{2+}$  and  $\text{Mn}^{2+}$  in  $\text{DMSO}:\text{H}_2\text{O}$  (8:2, v/v, 10 mM HEPES buffer, pH 7.4) solution at room temperature. As illustrated in Fig. 2, the free probe **L** displayed a maximal absorption peak at 345 nm which corresponds to  $\pi-\pi^*$  transition from the conjugated moiety of **L**. However, upon gradual addition of  $\text{Al}^{3+}$  ion to the solution of **L**, the initial absorption band at 345 nm decreased and a simultaneous increase at 402 nm with a red shift of 57 nm was observed, accompanied by a naked eye color change from colorless to light yellow. The clear isosbestic point at 370 nm undoubtedly indicates the formation of  $\text{Al}^{3+}$  complex in the binary mixture. Again, chemosensor **L** did not exhibit any noteworthy changes in absorption spectra with the addition of a number of competitive metal ions, signifying the high selectivity of this probe for  $\text{Al}^{3+}$  ion. To investigate the suitable pH range in which sensor, **L** can effectively detect  $\text{Al}^{3+}$ , a pH titration of **L** was carried out (Fig. S15, ESI<sup>†</sup>). It is noteworthy to mention that addition of  $\text{Al}^{3+}$  resulted in a high absorbance in a pH range of 6 to 9. When pH is greater than 9, the absorbance is decreased due to the formation of colloidal  $\text{Al}(\text{OH})_3$ . These observations indicate that the pH range of 6 to 9 is suitable for monitoring  $\text{Al}^{3+}$  by the chemosensor, **L**.

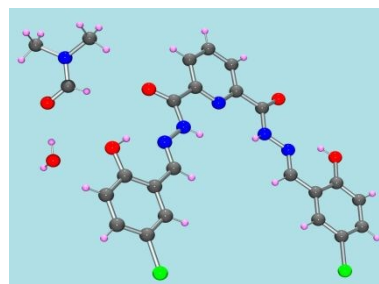


**Fig. 1** ORTEP view of molecular probe **L** (with 40% probability).

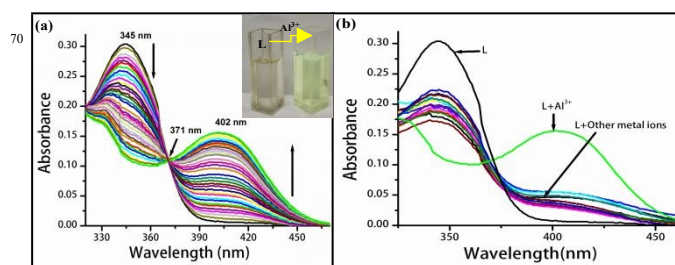


**Fig. 2** (a) The UV-vis absorption spectra of **L** ( $c = 2 \times 10^{-4}$  M) in presence of  $\text{Al}^{3+}$  ( $c = 2 \times 10^{-5}$  M) ions in  $\text{DMSO}:\text{H}_2\text{O}$  (8:2, v/v, 10 mM HEPES buffer, pH 7.4) solution. Inset: Color change after addition of  $\text{Al}^{3+}$  to probe **L**. (b) Absorption spectra of **L** in presence of different metal ions.

As shown in Fig. 3a, in absence of  $\text{Al}^{3+}$  ion, probe **L** showed a very weak emission band centred at 483 nm ( $\lambda_{\text{ext}} = 371$  nm) in  $\text{DMSO}:\text{H}_2\text{O}$  (8:2, v/v, 10 mM HEPES buffer, pH 7.4). This weak emission of probe **L** is due to the (a) excited state intramolecular

proton transfer (ESIPT) from the –OH group to the imine nitrogen; (b) photoinduced electron transfer effect from the lone pair of imine nitrogen and (c) isomerization of the –HC=N (imine) bond.<sup>26</sup> However, treatment of probe **L** with 3 equivalent  $\text{Al}^{3+}$  ions induced a gradual increase in fluorescence (20-fold) along with a blue shift of 7 nm having highest emission intensity at 476 nm and a color change from dark to greenish-blue under UV light. This significant fluorescence ‘turn-on’ in presence of  $\text{Al}^{3+}$  ions might be explicated by the formation of a complex between the probe **L** and  $\text{Al}^{3+}$  through the coordination of two “O” and one “N” atom. This inhibits both the ESIPT and PET processes as well as C=N isomerization resulting in a distinctive chelation enhanced fluorescence (CHEF) effect. In order to explore the practical applicability, the pH effects on the fluorescence response of probe **L** in absence and presence of  $\text{Al}^{3+}$  were examined. Fig. S16 shows that the **L** is weakly emissive in the wide range of pH (3-13). The low emission intensity of **L**- $\text{Al}^{3+}$  complex at pH < 6 was presumably due to the free **L** that remains uncoordinated to  $\text{Al}^{3+}$ . At pH > 9,  $\text{Al}^{3+}$  is converted to  $\text{Al}(\text{OH})_3$  and  $\text{Al}(\text{OH})_4^-$ , leaving the sensor almost in its free anionic form in the solution. At pH ~ 7 the sensor is deprotonated and the resulting dianionic ligand forms a chelate with  $\text{Al}^{3+}$ , leading to the fluorescence enhancement via CHEF mechanism (Scheme 2). Therefore, **L** sensor is capable of being used for selective detection of  $\text{Al}^{3+}$  at physiological pH, and can be a suitable candidate for biological applications.

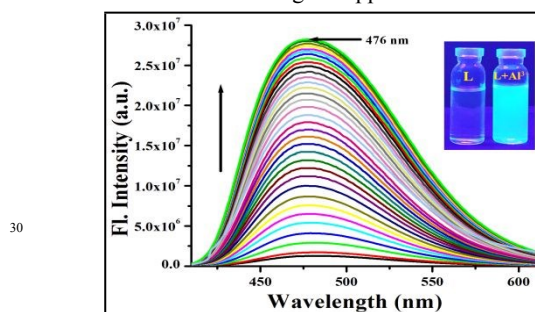


**Fig. 3** Changes in fluorescence spectra of **L** ( $c = 2 \times 10^{-4}$  M) in presence of different amount of  $\text{Al}^{3+}$  ( $c = 2 \times 10^{-5}$  M) ions in DMSO- $\text{H}_2\text{O}$  (8:2, v/v, 10 mM HEPES buffer, pH 7.4) solution. Inset: Fluorescence change after addition of  $\text{Al}^{3+}$  to probe **L**.

Additionally,  $^1\text{H}$  NMR titration was performed by gradual addition of nitrate salt of  $\text{Al}^{3+}$  ions to a DMSO- $d_6$  solution of **L** (Fig. 4).

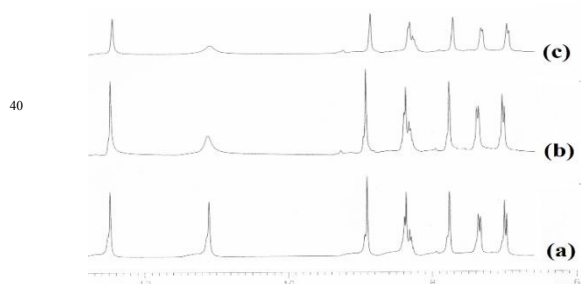


**Fig. 4**  $^1\text{H}$ NMR spectra in DMSO- $d_6$ : (a) **L** only (b) **L** and 1 equiv. of  $\text{Al}^{3+}$ (c) **L** and 2 equiv. of  $\text{Al}^{3+}$ .

The result shows that the intensity of the proton signal corresponding to the hydroxyl group (–OH) at 11.08 ppm, which is the most probable binding site for  $\text{Al}^{3+}$  ions, decreases significantly relative to that of other protons upon exposure to  $\text{Al}^{3+}$  ions.

For the chemosensor **L**, IR spectrum (Fig. S4, ESI) shows  $\nu(\text{OH})$ , 3472(s);  $\nu(\text{NH})$ , 3248(s);  $\nu(\text{C}=\text{O})$ , 1657(s);  $\nu(\text{C}=\text{N})$ , 1621  $\text{cm}^{-1}$ . On the other hand, IR spectrum of **L**- $\text{Al}^{3+}$  complex (Fig. S6, ESI) shows shifted frequency value and a new signal for  $\text{NO}_3^-$  at 1349  $\text{cm}^{-1}$ . The spectrum shows  $\nu(\text{NH})$ , 3189(s);  $\nu(\text{C}=\text{O})$ , 1672(s);  $\nu(\text{C}=\text{N})$ , 1617  $\text{cm}^{-1}$  but the  $\nu(\text{OH})$  appears as broad signal at 3449  $\text{cm}^{-1}$ . This result shows that the –OH is the most probable binding site for  $\text{Al}^{3+}$  ions.

The Job’s plot revealed that 1:2 stoichiometry is the most probable binding mode between **L** and  $\text{Al}^{3+}$  ions (Fig. S10, ESI $^\dagger$ ). To attain such type of stoichiometry, imine nitrogen, carbonyl oxygen and phenolic oxygen atoms are the most likely binding sites for  $\text{Al}^{3+}$  ions (Scheme 2). The association constant ( $K_a$ ) of **L** for  $\text{Al}^{3+}$  was calculated from the Benesi–Hildebrand equation<sup>27</sup> on the basis of fluorometric titration as  $4.26 \times 10^4$   $\text{M}^{-1}$  (Fig. S12, ESI $^\dagger$ ). The selectivity of chemosensor **L** towards different metal cations were examined under identical working conditions. As shown in Fig. 5, probe **L** demonstrated strong fluorescence response at 476 nm, while the other cations [ $\text{K}^+$ ,  $\text{Na}^+$ ,  $\text{Mg}^{2+}$ ,  $\text{Ca}^{2+}$ ,  $\text{Pb}^{2+}$ ,  $\text{Pd}^{2+}$ ,  $\text{Cd}^{2+}$ ,  $\text{Hg}^{2+}$ ,  $\text{Zn}^{2+}$ ,  $\text{Cu}^{2+}$ ,  $\text{Ag}^+$ ,  $\text{Fe}^{2+}$ ,  $\text{Co}^{2+}$ ,  $\text{Ni}^{2+}$  and  $\text{Mn}^{2+}$ ] did not cause any remarkable emission spectral changes. In order to further evaluate the practical capability of probe **L** as  $\text{Al}^{3+}$  selective fluorescent chemosensor, we conducted competitive experiments on addition of  $\text{Al}^{3+}$  ions to the solution of **L** in presence of excess equivalent of other individual competitive metal ions. The increase in fluorescence intensity induced by mixing  $\text{Al}^{3+}$  ions with other miscellaneous cations was comparable to that elicited by  $\text{Al}^{3+}$  alone, indicating stable complexation between **L** and  $\text{Al}^{3+}$ . The above results indicate high selectivity of probe **L** for  $\text{Al}^{3+}$  over other commonly coexistent cations in organo-aqueous solution. The fluorescence intensity of the **L** at 476 nm exhibited a good linear relationship with the  $\text{Al}^{3+}$  concentration ranging from 0.99  $\mu\text{M}$  to 20.6  $\mu\text{M}$ , based on which the detection limit<sup>28</sup> for  $\text{Al}^{3+}$  was calculated to be 0.8  $\mu\text{M}$  (Fig. S11, ESI $^\dagger$ ).

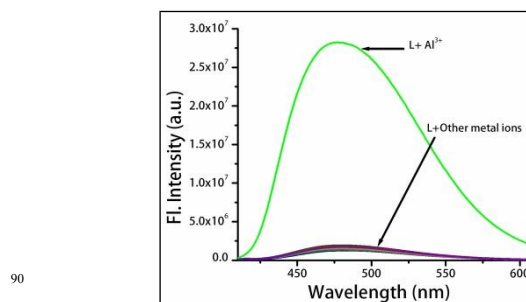


**Fig. 5** Fluorescence response of **L** ( $c = 2 \times 10^{-4}$  M) to different metal ions in DMSO- $\text{H}_2\text{O}$  (8:2, v/v, 10 mM HEPES buffer, pH 7.4) solution ( $\lambda_{\text{exc}} = 370$  nm).

Reversibility is an essential feature of a probe to be used as a chemosensor to detect particular metal cations. Here, the *in situ* generated  $L-2Al^{3+}$  complex displayed fluorescence “turn-off” behavior only in presence of  $HF_2^-$  ion. Now, to inspect this, when an excess amount of  $NaHF_2$  solution was added to the solution containing  $L-2Al^{3+}$  complex system, the emission band at 476 nm was gradually decreased, accompanied by the emission color changes from deep blue to dark (Fig. 6a). However, various common anions such as  $Cl^-$ ,  $Br^-$ ,  $AcO^-$ ,  $CO_3^{2-}$ ,  $N_3^-$ ,  $HCO_3^-$ ,  $NO_2^-$ ,  $SO_4^{2-}$ ,  $H_2PO_4^-$  did not produce any noticeable results under the similar conditions except  $F^-$ .  $F^-$  ion decreases the fluorescence intensity but only by a small extent compared to  $HF_2^-$  ion (Fig. 6b). The added fluoride source (TBAF) could be hydrolyzed, and a small amount of  $HF_2^-$  may be generated *in situ* to assist the quenching of emission of  $L-2Al^{3+}$  complex; thus, a quenching response might be observed.<sup>29</sup> Such fluorometric changes was mainly due to the removal of  $Al^{3+}$  from  $L-2Al^{3+}$  system followed by the regeneration of probe **L** as shown in **Scheme 2**. These properties indicate that  $L-2Al^{3+}$  ensemble is employed as an “on-off” fluorescent sensor for bifluoride ion. In addition, the reversible and reusable behavior of probe **L** was also verified by performing four alternate cycles of fluorescence titration of **L** with  $Al^{3+}$  followed by addition of  $HF_2^-$  as shown in Fig. S7 (ESI†). Moreover, from the fluorescence titration experiment, we found a good linear relationship of fluorescence intensity versus the  $HF_2^-$  concentration over a range of 0.99 to 6.5  $\mu M$  (Fig. S8, ESI†).

However, incremental addition of  $HF_2^-$  ion into the solution of *in situ* generated  $L-2Al^{3+}$  complex led to a gradual decrease in absorption band at 394 nm and a concomitant increase in the intensity of a new absorption band centered at 344 nm (Fig. S9, ESI†).

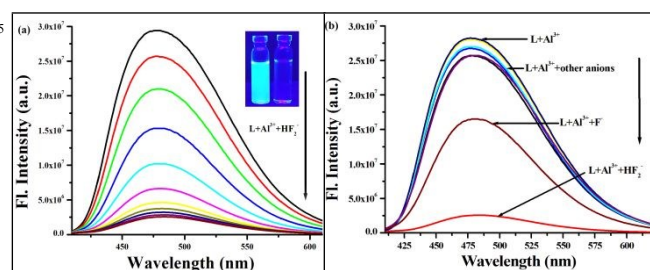
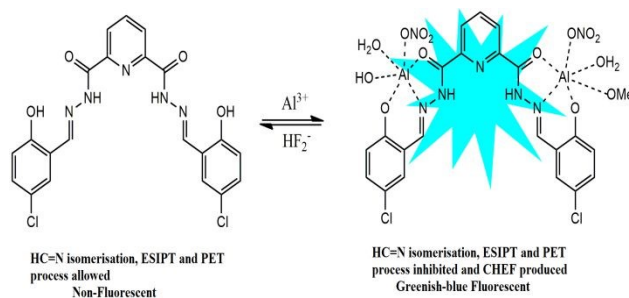


**Fig. 6** (a) Fluorescence titrations of  $L-2Al^{3+}$  complex with sodium salt of bifluoride in DMSO- $H_2O$  (8:2, v/v, 10 mM HEPES buffer, pH 7.4) solution ( $\lambda_{ext} = 370$  nm). Inset: Fluorescence photographs of  $L+Al^{3+}$  and  $L+Al^{3+}+HF_2^-$ . (b) Changes in the fluorescence spectra of  $L-2Al^{3+}$  complex in presence of different anions.



**Scheme 2** Proposed sensing mechanism for detection of  $Al^{3+}$  by probe **L**.

In order to know the optimized geometry of **L** and  $L-2Al^{3+}$  and the binding interactions between probe **L** and  $Al^{3+}$ , we carried out density functional theory (DFT) calculations with the B3LYP/6-311+G(d,p) basis set using the Gaussian 16 program.<sup>30,31</sup> The energy optimized structures of **L** and Al-complex were presented in Fig. 7. The highest occupied molecular orbital (HOMO), lowest unoccupied molecular orbital (LUMO) energies and spatial distribution of **L** and  $L-2Al^{3+}$  were also calculated (ESI†). As shown in Fig. 8, the HOMO-LUMO energy gap of probe **L** was considerably reduced from 3.83 eV (88.4 kcal/mol) to 3.16 eV (72.9 kcal/mol) in the  $L-2Al^{3+}$  complex, establishing that **L** formed stable complex with  $Al^{3+}$  ion and supports the red-shifting of the absorption band ( $\lambda_{max}$ ) in the UV-Vis absorption spectra.<sup>32</sup> Moreover TDDFT calculation were performed on the optimized geometries to explain the electronic properties of probe **L** and its Al-complex. Table S4 showed the details of the vertical excitation energies, oscillator frequencies and wavelengths and from these data it was found that the computed vertical transitions were analogous with the experimentally observed UV-vis bands.

The probe was applied in Hep G2 cells (Human liver cancer cell line) for fluorescence imaging of intracellular  $Al^{3+}$  ions to investigate its application in biological system. First, Hep G2 cells were treated with probe **L** (10  $\mu M$ ) for 30 min at 37°C and

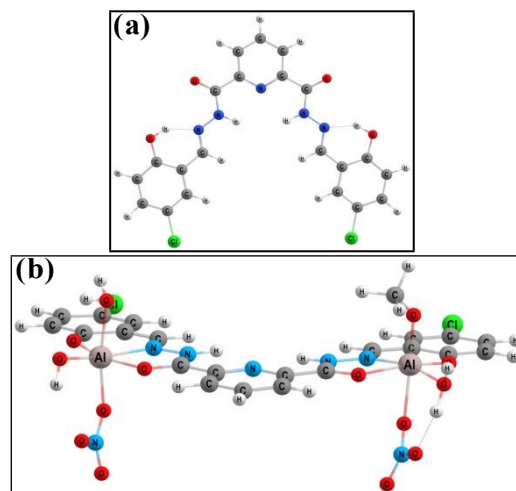


**Fig. 7** The calculated energy minimized structures of **L** and  $L-2Al^{3+}$  complex.

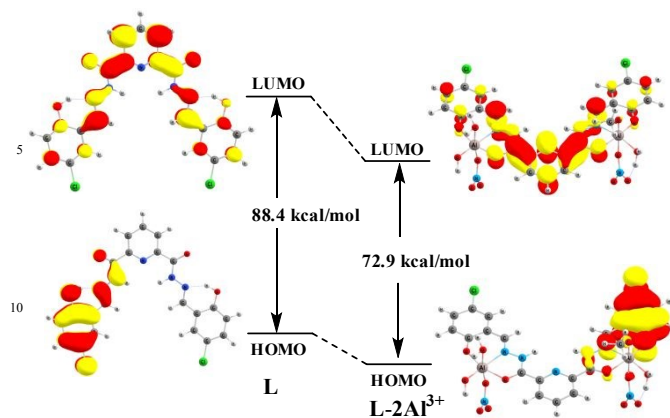


Fig. 8 HOMO and LUMO distributions of **L** and **L-2Al<sup>3+</sup>** complex.

then washed with PBS buffer to remove excess probe. After that, the treated cells were incubated with  $\text{Al}^{3+}$  ions ( $10 \mu\text{M}$ ) for another 30 min at  $37^\circ\text{C}$ . Then, these incubated cells were washed again with PBS buffer and images were recorded using a fluorescence microscope. Hep G2 cells treated with only probe **L** displayed no fluorescence signal, whereas an intense green fluorescence signal was detected in the intracellular area when stained with **L** followed by  $\text{Al}(\text{NO}_3)_3$ . Again, this bright fluorescence signal disappeared when the cells were treated with  $\text{NaHF}_2$  ( $10 \mu\text{M}$ ) solution (Fig. 9). Furthermore, there were no gross morphological changes in bright-field images of cells, suggesting that the cells remained viable throughout the imaging studies. The above results established the good cell-membrane permeability of **L** and that it could be employed in living cells for *in vitro* imaging of  $\text{Al}^{3+}$  and  $\text{HF}_2^-$  ions. Additionally, an MTT assay determined that probe **L** displayed very low cytotoxicity toward living cells (Fig. S14, ESI†).

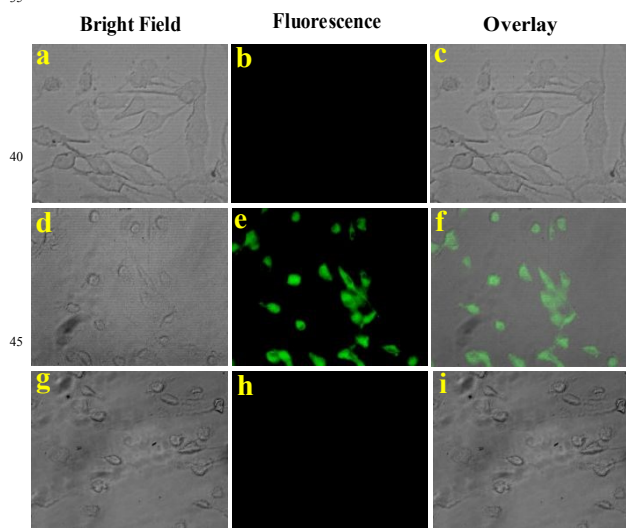


Fig. 9 Bright field, fluorescence and overlay images of Hep G2 cells. (a-c) cells were incubated with  $10 \mu\text{M}$  probe **L** for 30 min, (d-f) followed by addition and incubation with  $10 \mu\text{M}$   $\text{Al}^{3+}$  for another 30 min and (g-i) then with  $\text{NaHF}_2$  for 30 min.

## Conclusions:

In conclusion, we have successfully designed and synthesized a colorimetric and fluorometric probe, **L**, based on pyridine-dicarbohydrazide. The probe **L** shows both color and switch-on emission response to  $\text{Al}^{3+}$  ions in organo aqueous solution as a result of metal enhanced chelation effect (CHEF) inhibiting the PET, ESIPT and  $\text{C}=\text{N}$  isomerization processes. With a detection limit of  $0.8 \mu\text{M}$ , this chemosensor displays high selectivity for  $\text{Al}^{3+}$  ions over other 18 commonly coexistent metal ions. The stoichiometry of the **L**- $\text{Al}^{3+}$  is determined to be 1:2 (**L**:  $\text{Al}^{3+}$ ) and is confirmed by Job's plot analysis. The association constant for **L** with  $\text{Al}^{3+}$  is found to be  $4.26 \times 10^4 \text{ M}^{-1}$  on the basis of fluorescence studies, proposing a strong binding affinity for  $\text{Al}^{3+}$ . Besides, the *in situ* prepared **L-2Al<sup>3+</sup>** complex can be utilized for the detection of  $\text{HF}_2^-$  ions *via* the displacement approach and it exhibits a "turn-off" type of fluorescence response. Moreover, the detection of  $\text{Al}^{3+}$  and  $\text{HF}_2^-$  ions was also carried out in HepG2 cells to demonstrate the "off-on-off" fluorescence cellular image. It proves that molecule penetrates to cell and thus it is applicable to biological system. We anticipate that such type of cell imaging studies will be useful for  $\text{Al}^{3+}$  and  $\text{HF}_2^-$  ions related biological studies.

## Experimental Section

### Materials and apparatus:

All the chemical reagents and solvents (analytical and spectroscopic grades) were procured from commercial suppliers and used without additional purification. Millipore water was used throughout the experiment. Nitrate salts of  $\text{Al}^{3+}$  and  $\text{Ag}^+$ , chloride salts of metal ions ( $\text{Na}^+$ ,  $\text{K}^+$ ,  $\text{Cr}^{3+}$ ,  $\text{Cd}^{2+}$ ,  $\text{Fe}^{2+}$ ,  $\text{Zn}^{2+}$ ,  $\text{Hg}^{2+}$ ,  $\text{Pb}^{2+}$ ) and perchlorate salts of metal ions ( $\text{Ni}^{2+}$ ,  $\text{Mn}^{2+}$ ,  $\text{Cu}^{2+}$ ,  $\text{Fe}^{2+}$ ,  $\text{Co}^{2+}$ ), tetrabutyl ammonium salts of  $\text{F}^-$ ,  $\text{Br}^-$ ,  $\text{AcO}^-$ ,  $\text{HSO}_4^-$  and sodium salts of  $\text{HF}_2^-$ ,  $\text{PPI}$ ,  $\text{Pi}$ ,  $\text{NO}_3^-$  were used for the experiments. Elemental analyses (C, H and N) were performed using a PerkinElmer 2400 Series-II CHN analyzer, USA elemental analyzer. ESI mass spectra were obtained from a Water HRMS model XEVO-G2TOF#YCA351 spectrometer.  $^1\text{H}$  NMR and  $^{13}\text{C}$  NMR spectra were obtained from Bruker spectrometer ( $400 \text{ MHz}$ ) and  $^1\text{H}$  NMR titration spectra were obtained from Bruker spectrometer ( $300 \text{ MHz}$ ) with  $\text{DMSO-}d_6$  solvent using trimethylsilane (TMS) as an internal standard. Fourier transform infrared (FT-IR) spectra were recorded on a Perkin Elmer LX-1 FT-IR spectrophotometer ( $4000\text{--}400 \text{ cm}^{-1}$ ) by using a modern diamond attenuated total reflectance (ATR) accessory. UV-vis absorption spectra were obtained using UV-1700 PharmaSpec UV-vis spectrophotometer (SHIMADZU). Fluorescence emission spectra were carried out using a Horiba Jobin Yvon Fluoromax-4P spectrofluorometer. Single crystal structures (Fig. 1) were obtained using single-crystal X-ray diffractometer (Bruker Smart Apex II). The cells were imaged by using Zetasizer fluorescence microscope (Leica).

### Calculations for detection limit:

The detection limit of **L** for  $\text{Al}^{3+}$  was calculated using the following equation<sup>28</sup>:

$$\text{Detection limit} = 3\text{Sb1}/\text{S} \quad (1)$$

Where Sb1 is the standard deviation of the blank solution; and S is the slope of the calibration curve.

### Theoretical calculation:

All the geometries for **L** and  $\text{L-2Al}^{3+}$  were optimized by density functional theory (DFT) calculations using Gaussian 16 software package (basis set: B3LYP/6-31+G(*d,p*)). TDDFT calculation was also performed in the same level of theory.

### Cell imaging studies

#### Cell line culture

Human liver cancer cell line Hep G2 cells and Human lung fibroblast cells, WI-38 were collected from National Center for Cell Science (NCCS) Pune, India. The cells were grown in DMEM (Dulbecco's Modified Eagle Medium) with 10% FBS (Fetal Bovine Serum), penicillin/streptomycin (100units/ml) at 37°C and 5%  $\text{CO}_2$ . All the treatments were performed at 37°C and at a cell density allowing exponential growth.

#### Cell survivability assay

Cell survivability of the ligand were studied for human lung fibroblast cells, WI38 following reported procedure.<sup>33</sup> In brief, viability of WI-38 cells after exposure to various concentrations of probe **L** were assessed by MTT assay. The cells were seeded in 96-well plates at  $1 \times 10^4$  cells per well and exposed to probe **L** at concentrations of 0  $\mu\text{M}$ , 20  $\mu\text{M}$ , 40  $\mu\text{M}$ , 60  $\mu\text{M}$ , 80  $\mu\text{M}$ , 100  $\mu\text{M}$  for 24 hrs. After incubation cells were washed with 1×PBS twice and incubated with MTT solution (450 $\mu\text{g}/\text{ml}$ ) for 3-4 hrs at 37°C. The resulting formazan crystals were dissolved in an MTT solubilization buffer and the absorbance was measured at 570 nm by using a spectrophotometer (BioTek) and the value was compared with control cells.

#### Cellular Imaging

According to reported procedure, the Hep G2 cells were grown in a coverslip for more than 24h. Then, the Hep G2 cells were treated with 10 $\mu\text{M}$  of probe **L** for 30 min followed by addition and incubation with 10 $\mu\text{M}$   $\text{Al}(\text{NO}_3)_3$  solution and then with  $\text{NaHF}_2$  solution. The cells were washed with 1 X PBS. Lastly, they were then mounted on a glass slide and fluorescent images were taken from the Leica fluorescence microscope.

### Synthesis of Bis(2-hydroxy-4-chlorobenzaldehyde)-2,6-Pyridinedicarbohydrazone (**L**):

2,6-pyridinedicarbohydrazone was synthesized following reported method (**Scheme 1**).<sup>25</sup> A mixture of 2,6-pyridinedicarbohydrazone (0.19 g, 1.0 mmol) and 2-hydroxy-4-chlorobenzaldehyde (0.36 g, 2.3 mmol) was refluxed in methanol for 5 h. A light yellow solid formed was filtered off and dried in vacuum (yield 0.39 g (84%). m.p. > 200°C). Anal. Calc. for  $\text{C}_{21}\text{H}_{15}\text{Cl}_2\text{N}_5\text{O}_4$ , C 53.41, H 3.20, N 14.83. Found: C 54.12, H 4.01, N 15.23 %. <sup>1</sup>H NMR (400 MHz,  $\text{DMSO-}d_6$ ):  $\delta$  = 12.47 (s, 2H), 11.09 (s, 2H), 8.88 (s, 2H), 8.35 (d, *J* = 7.2 Hz, 2H), 8.28 (m, 1H), 7.92 (s, 3H), 7.75 (d, *J* = 2.4 Hz, 2H), 7.34 (m, 6.8 Hz, 2H), 6.97 (d, *J* = 8.8 Hz, 2H). <sup>13</sup>C NMR (100 MHz,  $\text{DMSO-}d_6$ ):  $\delta$  = 207.02 (for C=O of DMF), 162.79, 160.01, 156.46, 148.43, 147.17, 140.52, 131.64, 127.39, 126.22, 123.67, 121.48, 118.76, 31.17. IR (KBr,  $\text{cm}^{-1}$ ): 3472, 3248, 1657, 1621, 1538, 1481, 1353, 1264, 1187, 1089, 1000, 950, 824, 716, 608, 560. ESI-MS: *m/z* 472.11, calcd for  $[\text{C}_{21}\text{H}_{15}\text{Cl}_2\text{N}_5\text{O}_4 + \text{H}]^+$  472.06. Crystals suitable for X-ray structural determination were obtained by slow evaporation of DMF solution.

### Acknowledgements

Samit Pramanik thanks Council of Scientific and Industrial Research (CSIR, File no. 09/096(0947)/2018-EMR-I), New Delhi, for Junior Research Fellowship. The authors are thankful to Prof. Nitin Chattopadhyay and his scholar Mr. Sinjan Das of Department of Chemistry, Jadavpur University for instrumental facility. SKM and SP thank Haldia Government College for partial laboratory facility. DM is very much thankful to the DST, Government of India, for providing the INSPIRE Faculty Fellowship (DST/INSPIRE/04/2016/001948).

### Notes and references

- <sup>a</sup>Department of Chemistry, Jadavpur University, Kolkata 700032, India  
<sup>b</sup>Department of Chemistry, Haldia Government College, Debhog, Purba Medinipur, West Bengal, India  
<sup>c</sup>School of Chemistry and Biochemistry, Thapar Institute of Engineering and Technology, Patiala 147004, Punjab, India  
<sup>d</sup>Department of Life Science and Biotechnology, Jadavpur University, Kolkata 700032, India  
\*Sudipta Pathak, Tel: +91-8001317336.  
E-mails: [sudiptachemster@gmail.com](mailto:sudiptachemster@gmail.com)  
†Electronic Supplementary Information (ESI) available: CCDC 1979155 [details of any supplementary information available should be included here]. See DOI: 10.1039/b000000x/

### References

1. (a) S. Sen, T. Mukherjee, B. Chattopadhyay, A. Moirangthem, A. Basu, J. Marek and P. Chattopadhyay, *Analyst*, 2012, **137**, 3975–3981; (b) R. J. Lakowicz, *Principles of Fluorescence Spectroscopy*, 3rd ed.; Springer: New York, 2006; p xxvi; (c) A. P. de Silva, H. Q. N. Gunaratne, T. Gunlaugsson, A. J. M. Huxley, C. P. McCoy, J. T. Rademacher and T. E. Rice, *Chem.*

- 1  
2  
3  
4  
5  
6  
7  
8  
9  
10  
11  
12  
13  
14  
15  
16  
17  
18  
19  
20  
21  
22  
23  
24  
25  
26  
27  
28  
29  
30  
31  
32  
33  
34  
35  
36  
37  
38  
39  
40  
41  
42  
43  
44  
45  
46  
47  
48  
49  
50  
51  
52  
53  
54  
55  
56  
57  
58  
59  
60
- Rev., 1997, **97**, 1515–1566; (d) B. Valeur and I. Leray, *Coord. Chem. Rev.*, 2000, **205**, 3–40.
2. R. A. Yokel, *Food Chem. Toxicol.*, 2008, **46**, 2261–2266.
3. S. H. Kim, H. S. Choi, J. Kim, S. J. Lee, D. T. Quang and J. S. Kim, *Org. Lett.*, 2010, **12**, 560–563.
4. D. Krewski, R. A. Yokel, E. Nieboer, D. Borchelt, J. Cohen, J. Harry, S. Kacew, J. Lindsay, A. M. Mahfouz and V. Rondeau, *J. Toxicol. Environ. Health, Part B*, 2007, **10**, 1–269.
5. M. J. Cullen, M. J. Allwood, D. M. ambach, *Environ. Sci. Technol.*, 2012, **46**, 13048–13055.
6. (a) A. K. Mahapatra, S. S. Ali, K. Maiti, A. K. Manna, R. Maji, S. Mondal, M. R. Uddin, S. Mandal and P. A. Sahoo, *RSC Adv.*, 2015, **5**, 81203–81211; (b) T. Khan, S. Vaidya, D. S. Mhatre and A. Datta, *J. Phys. Chem. B*, 2016, **120**, 10319–10326.
7. (a) M. R. Wills and J. Savory, *Lancet*, 1983, **2**, 29–34; (b) C. A. Shaw and L. Tomljenovic, *Immunol. Res.*, 2013, **56**, 304–316; (c) G. Berthon, *Coord. Chem. Rev.*, 2002, **228**, 319–341.
8. (a) A. C. Alfrey, *Adv. Clin. Chem.*, 1983, **23**, 69–91; (b) A. M. Pierides, W. G. Edwards Jr, U. X. Cullum Jr, J. T McCall and H. A. Ellis, *Kidney Int.*, 1980, **18**, 115–124; (c) T. P. Flaten, *Brain Res. Bull.*, 2001, **55**, 187–196; (d) M. Yasui, T. Kihira and K. Ota, *Neurotoxicology*, 1992, **13**, 593–600; (e) P. Nayak, *Environ. Res.*, 2002, **89**, 101–115.
9. (a) B. Wang, W. Xing, Y. Zhao and X. Deng, *Environ. Toxicol. Pharmacol.*, 2010, **29**, 308–313; (b) P. D. Darbre, *J. Inorg. Biochem.*, 2005, **99**, 1912–1919.
10. (a) C. S. Cronan, W. J. Walker and P. R. Bloom, *Nature*, 1986, **324**, 140–143; (b) J. Barcelo and C. Poschenrieder, *Environ. Exp. Bot.*, 2002, **48**, 75–92.
11. V. Kumar, A. Kumar, U. Diwan, Ramesh Shweta, S.K. Srivastava, *Sens. Actuators, B*, 2015, **207**, 650–657.
12. M. Frankowski, A. Ziola-Frankowska, and J. Siepak, *Talanta*, 2010, **80**, 2120–2126.
13. G. Tangen, T. Wickstrom, S. Lierhagen, R. Vogt, W. Lund, *Environ. Sci. Technol.*, 2002, **36**, 5421–5425.
14. M. Rezaee, Y. Yamini, A. Khanchi, M. Faraji and A. Saleh, *J. Hazard. Mater.*, 2010, **178**, 766–770.
15. A. Sanz-Medel, A. B. Soldado Caabezuelo, R. Milačić and T. Bantan Polak, *Coord. Chem. Rev.*, 2002, **228**, 373–383.
16. Y. C. Chen, I. L. Lee, Y. M. Sung and S. P. Wu, *Talanta*, 2013, **117**, 70–74.
17. (a) V. K. Gupta, A. K. Jain and P. Kumar, *Sens. Actuators, B*, 2006, **120**, 259–265; (b) V. K. Gupta, B. Sethi, N. Upadhyay, S. Kumar, R. Singh and L. P. Singh, *Int. J. Electrochem. Sci.*, 2011, **6**, 650–663; (c) V. K. Gupta, R. Jain, and K. M. Pal, *Int. J. Electrochem. Sci.*, 2010, **5**, 1164–1178.
18. H. Wang, Z. Yu, Z. Wang, H. Hao, Y. Chen and P. Wan, *Electroanalysis*, 2011, **23**, 1095–1099.
19. (a) S. Samanta, B. Nath and J. B. Baruah, *Inorg. Chem. Commun.*, 2012, **22**, 98–100; (b) J. F. G. Reyes, P. O. Barrales, and A. M. Diaz, *Talanta*, 2005, **65**, 1203–1208.
20. (a) J. C. Qin, L. Fan, T. R. Li and Z. Y. Yang, *Synth. Met.*, 2015, **199**, 179–186; (b) S. Sinha, B. Chowdhury, and P. Ghosh, *Inorg. Chem.*, 2016, **55**, 9212–9220.
21. (a) A. Sahana, A. Banerjee, S. Lohar, B. Sarkar, S. K. Mukhopadhyay and Debasis Das, *Inorg. Chem.*, 2013, **52**, 3627–3633; (b) S. Kim, J. Y. Noh, K. Y. Kim, J. H. Kim, H. K. Kang, S.-W. Nam, S. H. Kim, S. Park, C. Kim and J. Kim, *Inorg. Chem.*, 2012, **51**, 3597–3602; (c) V. Saini, R. Krishnan and B. Khungar, *Photochem. Photobiol. Sci.*, 2020, DOI: 10.1039/C9PP00477G; (d) P. Ghorai, K. Pal, P. Karmakar and A. Saha, *Dalton Trans.*, 2020, **49**, 4758–4773.
22. M. Wang, C. Cheng, C. Li, D. Wu, J. Song, J. Wang, X. Zhou, H. Xiang and J. Liu, *J. Mater. Chem. C*, 2019, **7**, 6767–6778.
23. (a) K. Ashley, A. Agrawal, J. Cronin, J. Tonazzi, T. M. McCleskey, A. K. Burrell and D. S. Ehler, *Anal. Chim. Acta*, 2007, **584**, 281–286; (b) T. L. Peters, T. J. Nestrlick, L. L. Lamparski and R. H. Sthel, *Anal. Chem.*, 1982, **51**, 2397–2398; (c) C. R. Wade, A. E. J. Broomsgrove, S. Aldridge and F. o. P. Gabbai, *Chem. Rev.*, 2010, **110**, 3958–3984.
24. (a) K. Murugesan, V. Jeyasingh, S. Lakshminarayanan, S. Narayanan, S. Ramasamy, I. V. M. V. Enoch, and L. Piramuthu, *Spectrochim. Acta, Part A*, 2019, **209**, 165–169; (b) A. Ghorai, S. S. Thakur and G. K. Patra, *RSC Adv.*, 2016, **6**, 108717–108725; (c) K. Dutta, R. C. Deka, and D. K. Das, *J. Fluoresc.*, 2013, **23**, 823–828.
25. N. Yadav, A. K. Singh, *New J. Chem.*, 2018, **42**, 6023–6033.
26. (a) N. Xiao, L. Xie, X. Zhi and C. Fang, *Inorg. Chem. Commun.*, 2018, **89**, 13–17; (b) J. Wang and Y. Pang, *RSC Adv.*, 2014, **4**, 5845–5848; (c) S. K. Asthana, A. Kumar, Neeraj, Shweta, S. K. Hira, P. P. Manna, and K. K. Upadhyay, *Inorg. Chem. Commun.*, 2017, **56**, 3315–3323.
27. (a) C. Yang, L. Liu, T. W. Mu and Q.-X. Guo, *Anal. Sci.*, 2000, **16**, 537–539; (b) H. A. Benesi and J. H. Hildebrand, *J. Am. Chem. Soc.*, 1949, **71**, 2703–2707; (c) Y. Shiraishi, S. Sumiya, Y. Kohono and T. Hirai, *J. Org. Chem.*, 2008, **73**, 8571–8574.
28. (a) L. L. Long, D. D. Zhang, X. F. Li, J. F. Zhang, C. Zhang and L. P. Zhou, *Anal. Chim. Acta*, 2013, **775**, 100–105; (b) T. Mandal, A. Hossain, A. Dhara, A. A. Masum, S. Konar, S. K. Manna, S. K. Seth, S. Pathak and S. Mukhopadhyay, *Photochem. Photobiol. Sci.*, 2018, **17**, 1068–1074.
29. R. Purkait and C. Sinha, *New J. Chem.*, 2019, **43**, 9815–9823
30. (a) B. Miehllich, A. Savin, H. Stoll and H. Preuss, *Chem. Phys. Lett.*, 1989, **157**, 200–206; (b) A. D. Becke, *J. Chem. Phys.*, 1993, **98**, 5648–5662; (c) C. Lee, W. Yang and R. G. Parr, *Phys. Rev.*, 1988, **B37**, 785–799.
31. Gaussian 16, Revision C.01, M. J. Frisch, G. W. Trucks, H. B. Schlegel, G. E. Scuseria, M. A. Robb, J. R. Cheeseman, G. Scalmani, V. Barone, G. A. Petersson, H. Nakatsuji, X. Li, M. Caricato, A. V. Marenich, J. Bloino, B. G. Janesko, R. Gomperts, B. Mennucci, H. P. Hratchian, J. V. Ortiz, A. F. Izmaylov, J. L. Sonnenberg, -Y. D. Williams, F. Ding, F. Lipparini, F. Egidi, J. Goings, B. Peng, A. Petrone, T. Henderson, D. Ranasinghe, V. G. Zakrzewski, J. Gao, N. Rega, G. Zheng, W. Liang, M. Hada, M. Ehara, K. Toyota, R. Fukuda, J. Hasegawa, M. Ishida, T. Nakajima, Y. Honda, O. Kitao, H. Nakai, T. Vreven, K. Throssell, J. A. Jr. Montgomery, J. E. Peralta, F. Ogliaro, M. J. Bearpark, J. J. Heyd, E. N. Brothers, K. N. Kudin, V. N. Staroverov, T. A. Keith, R. Kobayashi, J. Normand, K. Raghavachari, A. P. Rendell, J. C. Burant, S. S. Iyengar, J. Tomasi, M. Cossi, J. M. Millam, M. Klene, C. Adamo, R. Cammi, J. W. Ochterski, R. L. Martin, K. Morokuma, O. Farkas, J. B. Foresman, D. J. Fox, Gaussian, Inc., Wallingford CT, 2016.

32. (a) R. Purkait, A. Dey, S. Dey, P. P. Ray, and C. Sinha, *New J. Chem.*, 2019, **43**, 14979–14990; (b) P. B. Thale, P. N. Borase and G. S. Shankarling, *Inorg. Chem. Front.*, 2016, **3**, 977–984.

33. (a) A. Samui, K. Pal, P. Karmakar and S. K. Sahu, *Mater. Sci. Eng. C*, 2019, **98**, 772–781; (b) K. Pal, S. Roy, P. K. Parida, A. Dutta, S. Bardhan, S. Das, K. Jana and P. Karmakar, *Mater. Sci. Eng. C*, 2019, **95**, 204–216.

## Table of Contents

### **Chromogenic and fluorogenic “off-on-off” chemosensor for selective and sensitive detection of aluminum ( $\text{Al}^{3+}$ ) and bifluoride ( $\text{HF}_2^-$ ) ions in solution and in living HepG2 cells: synthesis, experimental and theoretical studies**

Samit Pramanik,<sup>a</sup> Saikat Kumar Manna,<sup>b</sup> Sudipta Pathak,<sup>b,\*</sup> Debasish Mondal,<sup>c</sup> Kunal Pal,<sup>d</sup> and Subrata Mukhopadhyay<sup>a</sup>

<sup>a</sup>Department of Chemistry, Jadavpur University, Jadavpur, Kolkata, West Bengal, India

<sup>b</sup>Department of Chemistry, Haldia Government College, Debhog, Purba Medinipur, West Bengal, India

<sup>c</sup>School of Chemistry and Biochemistry, Thapar Institute of Engineering and Technology, Patiala - 147004, Punjab, India

<sup>d</sup>Department of Life Science and Biotechnology, Jadavpur University, Kolkata 700032, India

